

CAD model for circuit parameters of superconducting-based hybrid planar transmission lines

Hamid Reza Mohebbi and A Hamed Majedi

Integrated Quantum Optoelectronics Lab (IQOL), Department of ECE, Institute for Quantum Computing (IQC), University of Waterloo, Waterloo, N2L 3G1, Canada

E-mail: hmohebbi@maxwell.uwaterloo.ca and ahmajedi@maxwell.uwaterloo.ca

Received 3 June 2009, in final form 25 September 2009

Published 10 November 2009

Online at stacks.iop.org/SUST/22/125028

Abstract

Using the concept of surface impedance associated with a superconductor or normal conductor's plate, we extend the CAD (computer aided design) formalisms on modeling and simulation of superconducting and normal transmission lines (STL and NTL) in order to include hybrid transmission lines (HTL). STL and NTL are entirely made of superconductor or normal conductor materials, respectively. In this paper, HTL refers to a planar transmission line (TL) such as parallel plate (PPTL), microstrip (μ TL) and coplanar waveguide (CPW) whose ground plate is superconducting and whose top/center strip is a normal conductor or vice versa. We develop and present a set of closed-form equations in a tidy and succinct form for each configuration (STL, NTL and HTL) for widely-used planar TLs (PPTL, μ TL and CPW). They can be easily implemented in a systematic way by the user for the purpose of fast TL design. The results obtained with this CAD tool are compared with previously reported results in the literature, and good agreement is observed.

(Some figures in this article are in colour only in the electronic version)

1. Introduction

It is well known that the performance of TEM transmission lines (TL) in high-frequency circuits and systems can be enhanced by using superconductors. Superconducting transmission lines (STL) exhibit two predominate features: ultra-low loss and ultra-low dispersion [1, 2]. Cooper pairs are immune from the scattering process in superconductor materials, so a low resistance is observed. The origin of the non-dispersive behavior in superconductors is due to the fact that the penetration depth of the electromagnetic field through the superconductor is frequency independent, as opposed to the skin depth in metals. Superconductor TLs take advantage of an intrinsic property called kinetic inductance which is added to the series inductance associated to the line. This is because of the inertial mass associated with Cooper pairs in superconductor films. This extra kinetic inductance causes slow wave propagation [1]. On the other hand, due to the unique advantages of intrinsic accuracy and ultra-high sensitivity that superconductors offer, they are found as the basis for instrumentation, sensors and standards [3, 4].

Therefore, planar STL components can play an essential and instrumental role at every level of integration in microwave and THz integrated circuits for applications ranging from parametric devices [5, 6] to optoelectronic circuits [7, 8]. Recently, superconductor technology is one of the salient candidates for the implementation and realization of quantum information processors [9]. Since fast superconducting high-frequency circuits are one of the essential parts of such a computer system, the use of STL components becomes an attractive option.

Three prominent physical structures to construct planar TLs, particularly for miniaturized integrated circuits, are: parallel plate transmission lines (PPTL), microstrip lines (μ TL) and coplanar waveguides (CPW). Depending on the conductor type, one can assume three configurations for each planar TL: normal, superconducting and hybrid. In the normal transmission line (NTL) all conductor parts, including strips and ground plane, are made of normal conductors. In superconducting transmission lines (STL) all conductor plates are fabricated by superconductor materials. In the case of hybrid transmission lines (HTL) both types of conductors exist;

for instance, the strip part is a superconductor film and the ground plane is a normal metal plate. Incorporating these three configurations into the three types of TL, we realize nine combinations of these TLs.

Accurate, efficient and easy-to-use modeling of a planar TL comprising of superconductor materials is central to the development of many superconductor-based microwave circuits for the previously mentioned applications. Typically, an accurate evaluation of the characteristics for these circuits requires the use of full-wave electromagnetic solvers. However, this analysis is not well suited for rapid design and fast optimization purposes. Therefore, the need exists for a rigorous and complete computer aided design (CAD) formalism containing accurate closed-form expressions for circuit parameters of transmission lines compatible with superconductor technology.

For parallel plate transmission lines, as we explain shortly, the exact analytical formulation can be obtained for all configurations of NTL, STL and HTL. For microstrip and CPW transmission lines, composed of normal conductors, a rich and massive literature offering CAD or EDA (electronic design automation) formulae are available. These formulae form the main body of some commercial software, such as ADS (advanced design system), for the design of transmission lines. Some books are devoted to collecting all these formulae, in order to make an assessment over their accuracy and compare their range of validity [10–12]. However, there are few papers providing closed-form formulations of circuit parameters of superconducting microstrip and CPW transmission lines [13–15]. Derivation of the CAD formula, in NTLs and STL configuration of μ TL and CPW, are based on approximations in a quasi-TEM approach such as conformal mapping techniques [10, 16, 13] and asymptotic methods [17]. Some other CAD equations are acquired by numerical comparison and fitting the curves obtained from full-wave analysis [18–21].

To the best of our knowledge, there are a number of educational and commercial solvers for the simulation, design and optimization of superconductor-based circuits and TL components [22]. Educational software [23] is very limited and is not suitable for industrial-scale devices. User-friendly available products [24, 25] have been provided for those structures consisting of either perfect or normal conductors, and superconductor materials are usually not included in such software. More importantly, HTL which consists of both normal conductor and superconductor materials cannot be analyzed by these CAD or EDA software packages. In circuit simulators such as jSPICE, wrSPICE [26] and PSCAN [27] the Josephson junction element is included, but there is no access to the type and geometry of the transmission line components. With the concept of surface impedance, a full-wave analysis based on method of moment can be performed by SONNET [28] and Zeland IE3D [29], but it is not fast enough; in addition, one needs some pre-calculation to compare the real and imaginary parts of the surface impedance for normal and superconductor films. FastHenry and FastCap [30] are fast programs yielding the series inductance, resistance and shunt capacitance of a

transmission line based on mesh formation and boundary-element discretization techniques. However, the need to find the shunt conductance still remains to be calculated. In addition, writing input files to describe the geometry of the transmission line, including superconductor materials and also describing an inhomogeneous structure with different dielectric materials are the most difficult parts of these programs [31]. Moreover, when the problem under study contains distributed nonlinear media or lumped nonlinear circuit component, we need to modify the source code of the CAD tool to include the new nonlinear equation. This requires authority to access the source code of the CAD tool, as well as a knowledge of the procedure that the program follows, which is hardly achievable in commercial software.

Nonlinearity and the dispersive behavior of new materials can be easily included in the CAD tool that we present in this paper [32–34]. Although for NTL and STL configurations, closed-form expressions are reported, there are no closed-form equations for the circuit parameters of HTL. By employing the concept of surface impedance and energy calculation, we construct all the necessary equations describing HTL parameters for each aforementioned planar TL. Moreover, calculations of the internal inductance and resistance associated with NTL and STL, respectively, have been ignored in the set of available CAD equations. However, by the methodology that we proposed in this paper, they are provided and closed-form equations are obtained for both of them. Along the way, nine sets of CAD equations accommodating NTL, STL and HTL configurations for each PPTL, μ TL and CPW, are provided in a systematic way to be employed in developing a comprehensive CAD tool.

The rest of the paper is organized as follows. Section 2 of this paper describes the techniques that we used to find the circuit parameters of HTL, the internal inductance of NTL and the series resistance of STL. The surface impedances associated with the normal conductor and superconductor plate are given. Sections 3–5 are devoted to introducing all the closed-form equations for circuit parameters of all configurations of parallel plate, microstrip line and coplanar waveguide, respectively. The results of applying this CAD tool to some structures for design purposes are presented in section 6. The effects of the geometrical parameters on the electrical characteristics of TLs are also briefly discussed.

2. Methodology

2.1. Transmission line theory

A transmission line is usually referred to as a waveguide that can support only one single propagating mode (principal mode). If this principal mode is TEM, the voltage and current can be uniquely defined for this waveguide and distributed circuit theory can perfectly describe the behavior of the TL. In fact, TEM wave analysis and distributed circuit theory are two parallel approaches that are completely consistent in terms of describing the wave propagation through the TL. To support the ideal TEM mode, the TL must satisfy six conditions. First, the number of conductors should be two or

more [35], second the conductors should be perfect without any loss, third the media surrounding the conductors should be homogeneous [10], fourth the transverse dimension of the TL must be small enough with respect to the wavelength, fifth the frequency of the wave must be low enough in order not to excite higher order modes [36], and sixth the waveguide must be uniform along the direction of wave propagation. Therefore, realization of an ideal transmission line that can support a pure TEM wave is very difficult. However, in most practical case, the conductor loss is very small, so by simple perturbation analysis the effect of finite conductivity is captured and the TL picture remains valid [35, 10]. Inhomogeneous TLs, such as μ TLs, do not support a pure TEM mode of propagation except at zero frequency [10]. In this case, at low-frequency there exists a single dominant mode in the dispersion diagram [36, 37] close to the TEM mode which is referred to as a quasi-TEM mode.

2.2. Surface impedance

To find the circuit parameters associated with a TL, the conventional method is to begin by defining the voltage, current, charge and flux in terms of electric and magnetic fields or to use the energy approach as discussed in [10]. When the conductor plate is not perfect, the concept of surface impedance is very useful to define a boundary condition on the electric and magnetic field components [38–40]. The surface impedance of both a normal conductor and superconductor can be expressed by a complex number whose imaginary part is positive. The real part of this impedance represents the electric loss which manifests itself as a series resistance in the line and its positive imaginary part shows that both the normal conductor and superconductor are inductive. This kind of inductance is called the ‘internal inductance’ (or skin effect inductance), denoted by L_{int} , because it arises from the flux linkage internal to the conductor surface. For superconductor materials, the internal inductance is made up of two components: the penetration of the magnetic field into the superconductor and the kinetic energy of the superelectrons or Cooper pairs. In this paper, we call the total internal inductance in the superconductor films ‘kinetic inductance’, denoted by L_{kin} [1], and we leave the term internal inductance L_{int} , for normal conductor plates. The surface impedance associated with a conductor plate with thickness ‘ t ’ can be found by a transfer impedance formula from the bulk surface impedance [1, 41]. As a result, the real and imaginary parts of the surface impedance of a conductor plate can be found by the relations

$$R_{s,nc}^t = \frac{1}{2\delta_{nc}\sigma_{nc}} \frac{\sinh\left(\frac{2t}{\delta_{nc}}\right) + \sin\left(\frac{2t}{\delta_{nc}}\right)}{\sinh^2\left(\frac{t}{\delta_{nc}}\right) + \sin^2\left(\frac{t}{\delta_{nc}}\right)} \quad (1)$$

$$X_{s,nc}^t = \frac{1}{2\delta_{nc}\sigma_{nc}} \frac{\sinh\left(\frac{2t}{\delta_{nc}}\right) - \sin\left(\frac{2t}{\delta_{nc}}\right)}{\sinh^2\left(\frac{t}{\delta_{nc}}\right) + \sin^2\left(\frac{t}{\delta_{nc}}\right)} \quad (2)$$

$$R_{s,sc}^t = \frac{1}{\delta_{sc}\sigma_n} \left(\frac{\lambda_L}{\delta_{sc}}\right)^3 \frac{\sinh\left(\frac{2t}{\lambda_L}\right) + \left(\frac{\delta_{sc}}{\lambda_L}\right)^2 \sin\left(\frac{2t\lambda_L}{\delta_{sc}^2}\right)}{\sinh^2\left(\frac{t}{\lambda_L}\right) + \sin^2\left(\frac{t\lambda_L}{\delta_{sc}^2}\right)} \quad (3)$$

$$X_{s,sc}^t = \frac{1}{2}\omega\mu_0\lambda_L \frac{\sinh\left(\frac{2t}{\lambda_L}\right) - \left(\frac{\lambda_L}{\delta_{sc}}\right)^2 \sin\left(\frac{2t\lambda_L}{\delta_{sc}^2}\right)}{\sinh^2\left(\frac{t}{\lambda_L}\right) + \sin^2\left(\frac{t\lambda_L}{\delta_{sc}^2}\right)} \quad (4)$$

where $R_{s,nc}^t$, $X_{s,nc}^t$, $R_{s,sc}^t$ and $X_{s,sc}^t$ are the real and imaginary parts of the surface impedance of the superconductor film and normal conductor film with thickness t . In the above formulations, λ_L , σ_n , σ_{nc} , δ_{sc} and δ_{nc} are the London penetration depth of the superconductor plate, the conductivity of the normal channel of superconductor plate, the conductivity of the normal conductor plate, the skin depth of the superconductor in the normal channel and the skin depth of the normal conductor, respectively. Their relations and definitions are given by

$$\sigma_n(T) = \begin{cases} \sigma_0 & T \geq T_c \\ \sigma_0 \left(\frac{T}{T_c}\right)^\gamma & T \leq T_c \end{cases} \quad (5)$$

$$\lambda_L(T) = \begin{cases} \infty & T \geq T_c \\ \frac{\lambda_L(0)}{\sqrt{1 - \left(\frac{T}{T_c}\right)^\gamma}} & T \leq T_c \end{cases} \quad (6)$$

$$\delta_{sc}(\omega, T) = \sqrt{\frac{2}{\omega\mu_0\sigma_n(T)}} \quad (7)$$

$$\delta_{nc}(\omega, T) = \sqrt{\frac{2}{\omega\mu_0\sigma_{nc}}} \quad (8)$$

where σ_0 is the DC conductivity of the superconductor material just above its critical temperature, T_c , and $\lambda_L(0)$ is the penetration depth at zero temperature. The exponent parameter γ in (5) and (6) is a phenomenological parameter, which most of the time is considered as 2 for HTS and as 4 for LTS superconductor materials [42].

By using the concept of surface impedance, the stored time-averaged magnetic energy and power loss per unit length in the conductor plate of the TL can be calculated. This energy must be identical to its counterpart calculated by circuit theory, and this correspondence gives two equations [10, 43]

$$\frac{R_{nc}}{R_{s,nc}^t} = \frac{\omega L_{int}}{X_{s,nc}^t} \quad (9)$$

$$\frac{R_{sc}}{R_{s,sc}^t} = \frac{\omega L_{kin}}{X_{s,sc}^t}. \quad (10)$$

Equations (9) and (10) are very useful to find either the series kinetic/internal inductance or the series resistance counterpart when one of them is given by CAD formulation, as we use in this paper.

2.3. The procedure of finding circuit parameters

By solving Maxwell’s equations in a three-layer media it can be shown that most of the electrical energy in a typical planar TL is localized inside the dielectric media and there is a negligible amount of electrical energy stored inside the plates [44, 2]. This fact is also verified by having the non-negative imaginary

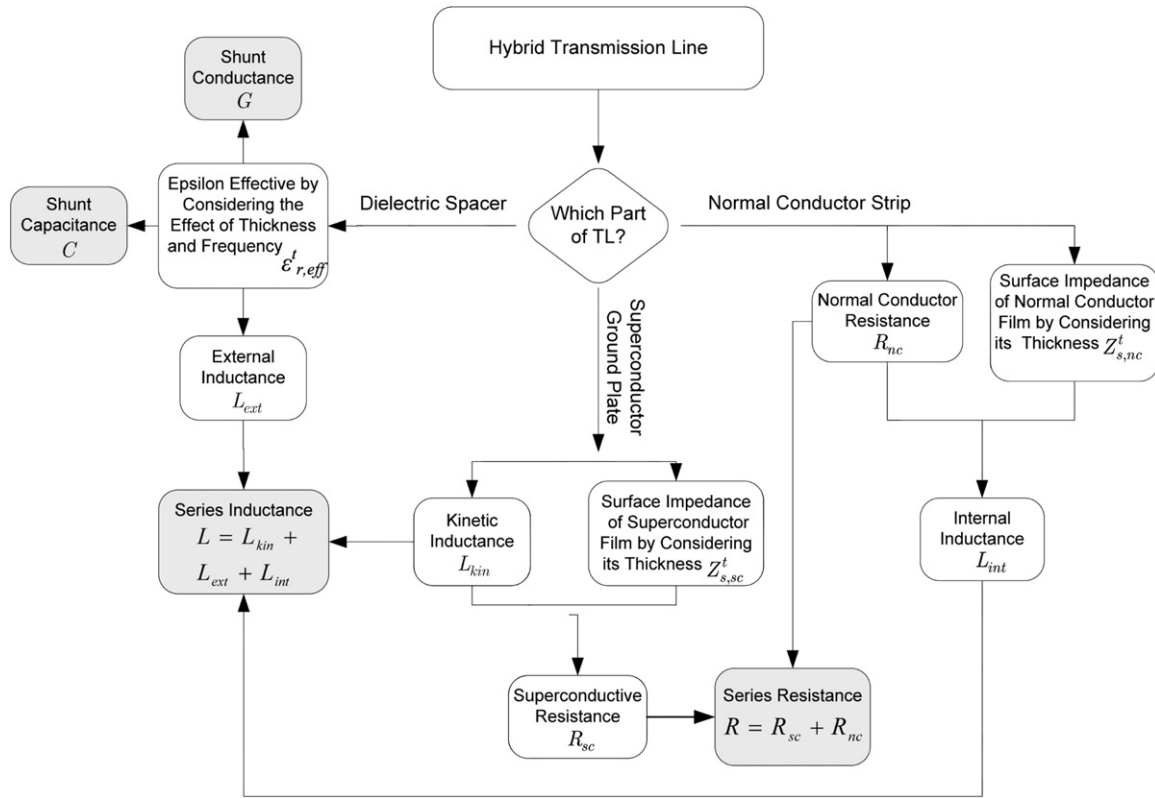


Figure 1. Flowchart for finding the circuit parameters of the hybrid conductor transmission line.

Table 1. Circuit parameters of all configurations of TLs.

	Total capacitance	Total inductance	Total resistance	Total conductance
Perfect conductor TL	C	L_{ext}	0	G
Superconducting TL	C	$L_{kin1} + L_{ext} + L_{kin2}$	$R_{sc1} + R_{sc2}$	G
Normal conductor TL	C	$L_{int1} + L_{ext} + L_{int2}$	$R_{nc1} + R_{nc2}$	G
Hybrid TL	C	$L_{int1} + L_{ext} + L_{kin2}$	$R_{nc1} + R_{sc2}$	G

part in the surface impedance associated with either the normal conductor or superconductor plate. Therefore, the capacitance per unit length for all three NTL, STL and HTL has to be the same as the case when perfect conductor plates exist.

Since magnetic energy can be found in both conductor and dielectric parts of the line, the total inductance per unit length is the summation of the external inductance and internal inductance. The inductance due to the magnetic field inside of the dielectric is usually called the ‘external inductance’ [10] denoted by L_{ext} , as it accounts for magnetic energy storage external to the conductors. It should be noted that by exchanging or swapping normal conductors with superconductors the external inductance remains unchanged, as the field distribution within the dielectric is only slightly affected. The total inductance per unit length for all configurations is shown in table 1. In this table index ‘1’ is used for one of the plates, for example the center strip or top plate and index ‘2’ is used for the ground or bottom plate.

When the dielectric material is lossy, the associated shunt conductance also remains the same for all above configurations of conductors, as long as they have the same dielectric spacer material.

Finite conductivity gives rise to the existence of a series resistance through the line. Because any transmission lines in this paper consist of two conductor plates (strip: 1, ground: 2), the total resistance of the line is the summation of these two components. Table 1 shows all the circuit parameters for all configurations of TL.

The procedure of finding circuit parameters of the HTL is depicted in the flowchart of figure 1 and calculation of the circuit parameters for other configurations can be performed in the same manner except that only one type of conductor needs to be considered.

3. Parallel plate transmission line (PPTL)

A parallel plate transmission line (PPTL) is a homogeneous waveguide with a planar structure, which can support all TE, TM and TEM modes, depending on the height of the dielectric spacer and the frequency of wave propagation. If the amount of conductor loss is small, which is the case in superconductive and good conductor plates, the longitudinal component of the electric field is so small that it can be ignored. In this case the

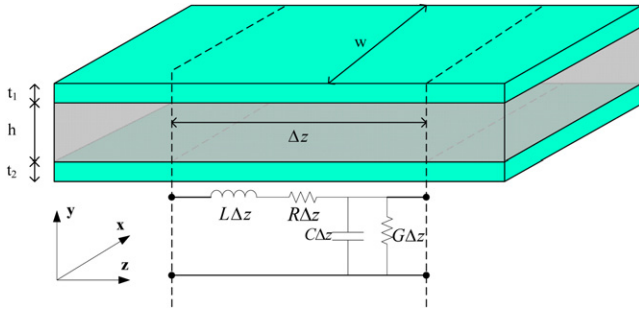


Figure 2. Parallel plate transmission line.

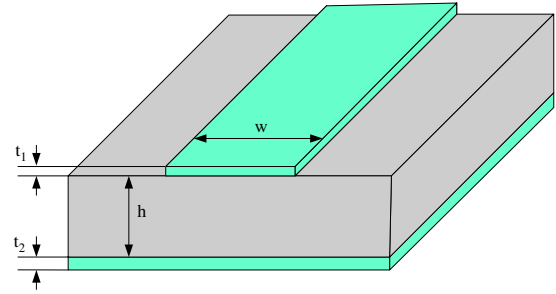


Figure 3. A typical microstrip line.

quasi-TEM approximation can be applied to find distributed circuit parameters [1, 2, 22, 45–49]. Fortunately, analytical closed-form expressions can be found for all NTL, STL and HTL configurations of parallel plate transmission lines, as we discuss in this section.

A typical parallel plate transmission line is shown in figure 2. The width w of the line is assumed large enough, compared to the wavelength of the wave, to form a homogeneous TL to support a TEM wave. The capacitance and conductance due to the dielectric loss will be the same for all different combinations of conductor materials:

$$C = \epsilon_0 \epsilon_{rd} \frac{w}{h} \quad (11)$$

$$G = C \frac{\sigma_d}{\epsilon_0 \epsilon_{rd}} = C \omega \tan \delta \quad (12)$$

where ϵ_{rd} is the dielectric constant (real part) of the dielectric spacer, ω is the frequency of operation, σ_d is the conductivity of the dielectric material and $\tan \delta$ is the loss tangent which is defined later in equation (51). The kinetic and internal inductance for each plate and external inductance are also found [2]:

$$L_{ext} = \frac{\mu_0 h}{w} \quad (13)$$

$$L_{kin} = \frac{\mu_0 \lambda_L}{w} \coth \frac{t}{\lambda_L} \quad (14)$$

$$L_{int} = \frac{\mu_0 \delta_{nc}}{4w} \frac{\sinh(\frac{2t}{\delta_{nc}}) - \sin(\frac{2t}{\delta_{nc}})}{\sinh^2(\frac{t}{\delta_{nc}}) + \sin^2(\frac{t}{\delta_{nc}})} \quad (15)$$

The resistance per unit length associated with a single ohmic metal and superconductor can be found by using equations (9) and (10), which returns the same equations found by the energy relation in [2]:

$$R_{sc} = \frac{1}{w \delta_{sc} \sigma_n} \left(\frac{\lambda_L}{\delta_{sc}} \right)^3 \frac{\sinh(\frac{2t}{\lambda_L}) + (\frac{\delta_{sc}}{\lambda_L})^2 \sin(\frac{2t \lambda_L}{\delta_{sc}^2})}{\sinh^2(\frac{t}{\lambda_L}) + \sin^2(\frac{t \lambda_L}{\delta_{sc}^2})} \quad (16)$$

$$R_{nc} = \frac{1}{2w \delta_{nc} \sigma_n} \frac{\sinh(\frac{2t}{\delta_{nc}}) + \sin(\frac{2t}{\delta_{nc}})}{\sinh^2(\frac{t}{\delta_{nc}}) + \sin^2(\frac{t}{\delta_{nc}})} \quad (17)$$

Now by using equations (11)–(17), table 1 and the procedure illustrated in the flowchart of figure 1, one can find the total circuit parameters of all three configurations of the parallel plate transmission line.

4. Microstrip line (μ TL)

Of the various transmission line structures used in microwave designs, the microstrip line is probably the most popular one because of its simple geometry, small size, scalability and possible integration with various passive and active devices. In the 1960s and 1970s microstrip lines found remarkable applications and they have been regarded as an essential element in microwave integrated circuits. Therefore, extensive research was carried out to analyze and model this kind of transmission line [50]. As mentioned in section 2.1, unlike the parallel plate transmission line, the microstrip line is an inhomogeneous structure with a quasi-TEM as the dominant mode of propagation. The operating frequency must be low enough in order not to violate the single mode of propagation.

For the superconducting microstrip line depicted in figure 3, the kinetic inductance per unit length is chosen from [13]. This work is based on calculating the fringing field factor $K(w, h, t_1)$. This is the factor by which the width of the strip appears to be increased; therefore, reducing the magnetic field. This factor can be expressed in terms of the ‘aspect ratio’ $u = w/h$ and ‘normalized strip thickness’ $t_h = t_1/h$.

Indeed, both the finite width and thickness of the conductor give rise to a field fringe, and these two sources have been considered in [13] to calculate the fringe factor. The formula presented in [13] gives an accurate external and kinetic inductance when the aspect ratio of the μ TL exceeds unity ($w > h$). The fringe factor $K(u, t_h)$ can be found through the following relations

$$K(u, t_h) = \frac{2}{\pi u} [\ln(2r_b) - \ln(r_a)] \quad (18)$$

where

$$r_b = \begin{cases} r_{b0} = q + \frac{p+1}{2} \ln(D) & 5 \leq u \\ r_{b0} - \sqrt{(r_{b0}-1)(r_{b0}-p)} \\ + (p+1) \tanh^{-1} \left(\frac{r_{b0}-p}{r_{b0}-1} \right)^{1/2} \\ - 2\sqrt{p} \tanh^{-1} \left(\frac{r_{b0}-p}{p(r_{b0}-1)} \right)^{1/2} \\ + \frac{\pi}{2} u \sqrt{p} & 1 \leq u \leq 5 \end{cases} \quad (19)$$

$$\ln(r_a) = -1 - \frac{\pi}{2}u + \ln(4p) - \frac{(\sqrt{p} + 1)^{1/2}}{2\sqrt{p}} \ln(\sqrt{p} + 1) + \frac{(\sqrt{p} - 1)^{1/2}}{2\sqrt{p}} \ln(\sqrt{p} - 1) \quad (20)$$

$$D = \text{Max}\{p, q\} \quad (21)$$

$$q = \frac{\pi}{2}u\sqrt{p} + \frac{p+1}{2} \left[1 + \ln\left(\frac{4}{\sqrt{p}+1}\right) \right] - \sqrt{p} \ln(\sqrt{p} + 1) - \frac{(\sqrt{p} - 1)^2}{2} \ln(\sqrt{p} - 1) \quad (22)$$

$$p = 2(1 + t_h)^2 - 1 + \sqrt{[2(1 + t_h)^2 - 1]^2 - 1}. \quad (23)$$

The external inductance and kinetic inductance due to penetration of the magnetic field into the superconducting strip and ground plane are:

$$L_{\text{kin1}} = \frac{\mu_0 \lambda_{L1}}{wK(u, t_h)} \left[\coth\left(\frac{t_1}{\lambda_{L1}}\right) + \frac{2\sqrt{p}}{r_b} \text{csch}\left(\frac{t_1}{\lambda_{L1}}\right) \right] \quad (24)$$

$$L_{\text{kin2}} = \frac{\mu_0 \lambda_{L2}}{wK(u, t_h)} \coth\left(\frac{t_2}{\lambda_{L2}}\right) \quad (25)$$

$$L_{\text{ext}} = \frac{\mu_0 h}{wK(u, t_h)} \quad (26)$$

where λ_{L1} and λ_{L2} are the penetration depths for superconductor materials of which the strip and ground plane are made, respectively. Equation (25) is similar to (14) for the associated kinetic inductance of a superconductive plate in a parallel plate transmission line. The total inductance for each type of transmission line can be found by looking at table 1.

As described previously, the shunt capacitance and conductance should be the same as in the case of a perfect conductor. The characteristic impedance and capacitance per unit length of the line require an effective dielectric constant. To find the effective dielectric constant, we use the quasi-static formulae in [18], since it seems more accurate for a wide range of geometries and dielectric constant. The error of this model is less than 0.2% for $\epsilon_r \leq 128$ and $0.01 \leq u \leq 100$ [18]. However, as will be shown later, it needs to be modified to consider the effect of conductor thickness and dispersion due to frequency variation as [18]

$$a(u) = 1 + \frac{1}{49} \ln\left(\frac{u^4 + (\frac{u}{52})^2}{u^4 + 0.432}\right) + \frac{1}{18.7} \ln\left[1 + \left(\frac{u}{18.1}\right)^3\right] \quad (27)$$

$$b(\epsilon_{rd}) = 0.564 \left(\frac{\epsilon_{rd} - 0.9}{\epsilon_{rd} + 3}\right)^{0.053} \quad (28)$$

$$\epsilon_{\text{ref}}(0) = \frac{\epsilon_{rd} + 1}{2} + \frac{\epsilon_{rd} - 1}{2} \left(1 + \frac{10}{u}\right)^{-a(u)b(\epsilon_{rd})}. \quad (29)$$

This effective dielectric constant is for the case of infinitely thin strip plates. The finite thickness t_1 , causes the electric field to spread from the edges of the strip. The effect of this fringing field is accounted for by calculating an effective strip width of zero thickness that would produce an electric field having the same width as that produced by the μ TL having a finite conductor thickness. This effective width is different from $wK(u, t_h)$, because that was formulated based on the

magnetic field to find the inductance, but this effective width is calculated based on fringing of the electric field to find the capacitance of the line. By defining an effective aspect ratio $u_e = w_e/h$, a simple formula for this purpose is given in [10]

$$u_e = \begin{cases} u + \frac{1.25}{\pi} t_h \left[1 + \ln\left(\frac{4\pi u}{t_h}\right) \right] & u \leq \frac{1}{2\pi} \\ u + \frac{1.25}{\pi} t_h \left[1 + \ln\left(\frac{2}{t_h}\right) \right] & u \geq \frac{1}{2\pi}. \end{cases} \quad (30)$$

The above effective aspect ratio u_e can be used in equations (27)–(29), instead of u , to evaluate the effective dielectric constant with thickness correction. Due to the inhomogeneity in a microstrip line, dispersion can impose a strong effect on wave propagation. Typically as the frequency increases, the effective dielectric constant ϵ_{ref} increases in a nonlinear manner, approaching an asymptotic value [11, 12]. We combined two different formulations [21, 51] to cover a wider range of accuracy, as follows. If $0.1 < u < 10$, we implement the CAD formula reported in [21] as stated below

$$\epsilon_{\text{ref}}^t(f) = \epsilon_{rd} - \frac{\epsilon_{rd} - \epsilon_{\text{ref}}^t(0)}{1 + (\frac{f}{f_{50}})^m} \quad (31)$$

$$f_{50} = \frac{f_{k, \text{TM}_0}}{0.75 + (0.75 - \frac{0.332}{\epsilon_{rd}^{1.73}})u} \quad (32)$$

$$f_{k, \text{TM}_0} = \frac{c_0 \tan^{-1}\left(\epsilon_{rd} \sqrt{\frac{\epsilon_{\text{ref}}^t(0) - 1}{\epsilon_{rd} - \epsilon_{\text{ref}}^t(0)}}\right)}{2\pi h \sqrt{\epsilon_{rd} - \epsilon_{\text{ref}}^t(0)}} \quad (33)$$

$$m_0 = 1 + \frac{1}{1 + \sqrt{u}} + 0.32 \left(\frac{1}{1 + \sqrt{u}}\right)^3 \quad (34)$$

$$m_c = \begin{cases} 1 + \frac{1.4}{1 + u} \{0.15 - 0.235 e^{-\frac{0.45f}{f_{50}}}\} & u \leq 0.7 \\ 1 & 0.7 < u \end{cases} \quad (35)$$

$$m = m_0 m_c \quad (36)$$

where c_0 is the speed of electromagnetic wave in free space. If $10 < u < 100$, we use the formulation in [52]

$$\epsilon_{\text{ref}}^t(f) = \epsilon_{rd} - \frac{\epsilon_{rd} - \epsilon_{\text{ref}}^t(0)}{1 + P(f)} \quad (37)$$

$$P(f) = P_1 P_2 [(0.1844 + P_3 P_4) f_n]^{1.5763} \quad (38)$$

$$P_1 = 0.27488 + u \left(0.6315 + \frac{0.525}{(1 + 0.0157 f_n)^{20}}\right) - 0.065683 e^{-8.7513u} \quad (39)$$

$$P_2 = 0.33622(1 - e^{-0.03442\epsilon_{rd}}) \quad (40)$$

$$P_3 = 0.0363 e^{-4.6u} [1 - e^{-\left(\frac{f_n}{38.7}\right)^{4.97}}] \quad (41)$$

$$P_4 = 1 + 2.751 [1 - e^{-\left(\frac{\epsilon_{rd}}{15.916}\right)^8}] \quad (42)$$

$$f_n = \frac{fh}{10^6} \text{ (GHz mm)}. \quad (43)$$

The definition of the effective dielectric constant is as follows

$$\epsilon_{\text{ref}}^t = \frac{C}{C_{\text{air}}} = \frac{c_0}{v_p} \quad (44)$$

where c_0 is the speed of light in free space, v_p is the phase velocity of the propagating wave, C_{air} is the capacitance per length for the line when it is filled by air and C is the real capacitance per length for the line. According to [17] and using equation (44), the capacitance per unit length will be

$$C = \epsilon'_{ref}(f)\epsilon_0 \left\{ u^n + \left[2\pi \left[\frac{1}{\ln\left(\frac{8}{u} + 1\right)} - \frac{u}{8} \right] \right]^n \right\}^{\frac{1}{n}} \quad (45)$$

where $n = 1.07$.

As the contribution of each part of the TL, i.e. dielectric, strip, and ground plane in kinetic inductance is clearly delineated in [13], by equations (26)–(28), the associated resistance for each plate can be found through equations (9) and (10); then the total resistance can be found by using table 1.

For normal conductors, the power loss and series resistance can also be evaluated using conformal mapping techniques. The associated series resistance for the strip and ground plane is [10]

$$R_{nc1} = \frac{R'_{s,nc1}}{w} \times LR \times \left[\frac{1}{\pi} + \frac{1}{\pi^2} \ln\left(\frac{4\pi w}{t}\right) \right] \quad (46)$$

$$R_{nc2} = \frac{R'_{s,nc2}}{w + 5.8h + 0.03\frac{h}{u}} \quad (47)$$

respectively. Equations (46) and (47) have a better accuracy when $0.1 \leq u \leq 10$ [10]. The surface resistance for the strip with thickness t_1 and the ground plane with thickness t_2 denoted by $R'_{s,nc1}$ and $R'_{s,nc2}$ can be found by equations (1) and (2). LR is a parameter which called the ‘loss ratio’ that can be evaluated by this equation

$$LR = \begin{cases} 1 & u \leq 0.5 \\ 0.94 + 0.132u - 0.0062u^2 & 0.5 < u \leq 10. \end{cases} \quad (48)$$

The internal inductance of the normal conductor (skin effect inductance) which accounts for the penetration of magnetic field into the conductors can be easily evaluated by knowing the series resistance associated with each conductor and using (9) and (10). Hence, the total inductance of the normal microstrip line can be found by using table 1.

When the dielectric is lossy with nonzero conductivity σ_d , the shunt conductance is given by the equation below for a microstrip transmission line

$$G = \omega q C \tan \delta \quad (49)$$

where C is the capacitance per unit length. This equation is similar to (12), which is used to calculate the capacitance of a parallel plate transmission line, except that it has been multiplied by factor ‘ q ’. The parameter ‘ q ’ is called the ‘filling factor’ and intuitively is the portion of the microstrip line’s cross section that is not filled by air. The filling factor and loss tangent are defined by the relation

$$q = \frac{\epsilon'_r}{\epsilon_{ref}} \times \frac{\epsilon_{ref} - 1}{\epsilon'_r - 1} \quad (50)$$

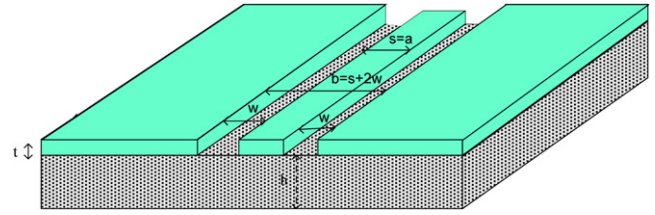


Figure 4. CPW transmission line.

$$\tan \delta = \frac{\epsilon''_r}{\epsilon'_r} \quad (51)$$

where $\hat{\epsilon}_r = \epsilon'_r - j\epsilon''_r = \epsilon_{rd} - j(\sigma_d/\omega\epsilon_0)$ is the complex permittivity of the dielectric section. The effective dielectric constant ϵ_{ref} can be chosen from (31) and (37) as a thickness and dispersion correction has been applied.

5. Coplanar waveguide (CPW)

Coplanar waveguides can be thought as a coupled slotline. The signal is applied to the center strip conductor with two ground planes on either side. A CPW can be designed in applications when a high characteristic impedance is required. On the other hand, μ TLs are used when low characteristic impedance is demanded [11]. The dominant mode of propagation resembles quasi-TEM, but at higher frequencies the field becomes non-TEM. Nonetheless, in many integrated microwave circuit applications, the line dimensions are so small relative to the wavelength that quasi-TEM analysis can be used [10]. Indeed, there are various configurations for coplanar waveguides [53], and in this work we study the ‘conventional CPW’ where the ground plane is of semi-infinite extent on either side. Fortunately, like the μ TL, CAD formulae are available for both normal and superconducting CPW [11, 12, 53]. If a CPW consists of normal conductors, the associated series resistance for the center conductor and ground plane can be found in [10]. Similar to the μ TL, the corresponding internal inductance for each metal section can be evaluated by (9) and (10). The contribution of the center strip and the ground plane to the kinetic inductance can be written separately. This separation is very helpful to find the associated series resistance of hybrid CPW as given by table 1.

Geometrical parameters related to a typical CPW are illustrated in figure 4. As mentioned before, shunt conductance and capacitance do not change for either the normal or superconducting state in all types of transmission lines. In CPWs, the capacitance per length is given by [53]

$$C = 2\epsilon_0(\epsilon_{rd} - 1) \frac{K(k_1)}{K(k'_1)} + 4\epsilon_0 \frac{K(k_0)}{K(k'_0)} \quad (52)$$

where $K(k_0)$ is the complete elliptical integral of the first kind and parameters k_0, k'_0, k_1 and k'_1 are defined by the relations

$$k_0 = \frac{s}{s + 2w} \quad (53)$$

$$k'_0 = \sqrt{1 - k_0^2} \quad (54)$$

$$k_1 = \frac{\sinh\left(\frac{\pi s}{4h}\right)}{\sinh\left[\frac{\pi(s+2w)}{4h}\right]} \quad (55)$$

$$k'_1 = \sqrt{1 - k_1^2}. \quad (56)$$

Similar to the microstrip line, k_0 is called the 'aspect ratio'. The following equations give the 'filling factor' and also the 'effective dielectric constant' for a CPW which usually have to be defined for an inhomogeneous transmission line

$$q = \frac{1}{2} \frac{K(k_1)K(k'_0)}{K(k'_1)K(k_0)} \quad (57)$$

$$\varepsilon_{\text{ref}}(0) = 1 + q(\varepsilon_{\text{rd}} - 1) \quad (58)$$

where $\varepsilon_{\text{ref}}(0)$ is the effective dielectric constant for a zero thickness conductor at zero frequency. In a manner similar to the microstrip case, this effective dielectric constant should be modified because of the finite thickness of the strips and dispersion behavior of the line. The effect of metallization thickness on $\varepsilon_{\text{ref}}(0)$ can be taken into account by the following empirical relations [12]

$$\varepsilon_{\text{ref}}^t(0) = \varepsilon_{\text{ref}}(0) - \frac{0.7[\varepsilon_{\text{ref}}(0) - 1]\frac{t}{w}}{\frac{K(k_0)}{K'(k_0)} + 0.7\frac{t}{w}}. \quad (59)$$

The frequency dependent effective dielectric constant has been presented in [54] by a closed-form expression, as follows

$$\sqrt{\varepsilon_{\text{ref}}^t(f)} = \sqrt{\varepsilon_{\text{ref}}^t(0)} + \frac{\sqrt{\varepsilon_{\text{rd}}} - \sqrt{\varepsilon_{\text{ref}}^t(0)}}{1 + g\left(\frac{f}{f_{\text{TE}}}\right)^{-1.8}} \quad (60)$$

$$g = e^{u \ln\left(\frac{s}{w}\right) + v} \quad (61)$$

$$f_{\text{TE}} = \frac{c_0}{4h\sqrt{\varepsilon_{\text{rd}} - 1}} \quad (62)$$

$$u = 0.54 - 0.64p + 0.015p^2 \quad (63)$$

$$v = 0.43 - 0.86p + 0.54p^2 \quad (64)$$

$$p = \ln\left(\frac{s}{h}\right) \quad (65)$$

where c_0 is the speed of light in free space. The error of this model is claimed to be around 5%, when $0.1 < w/h < 5$, $1.5 < \varepsilon_{\text{r}} < 50$, $0.1 < s/w < 5$ and $0 < f/f_{\text{TE}} < 10$ [54].

If a CPW consists of normal conductors, the associated series resistance for the center conductor and ground plane can be found by [10]

$$R_{\text{nc1}} = \frac{R_{\text{s,nc1}}^t}{4s(1 - k_0^2)K^2(k_0)} \left[\pi + \ln\left(\frac{4\pi s}{t}\right) - k_0 \ln\left(\frac{1 + k_0}{1 - k_0}\right) \right] \quad (66)$$

$$R_{\text{nc2}} = \frac{k_0 R_{\text{s,nc1}}^t}{4s(1 - k_0^2)K^2(k_0)} \times \left[\pi + \ln\left(\frac{4\pi(s + 2w)}{t}\right) - \frac{1}{k_0} \ln\left(\frac{1 + k_0}{1 - k_0}\right) \right] \quad (67)$$

where $R_{\text{s,nc}}^t$ and k_0 are the surface resistance for a normal conductor with thickness t , and the aspect ratio respectively.

The corresponding internal inductance for each metal section can be evaluated by equations (9) and (10).

The kinetic inductance per unit length is given by [14] and [55] by using the conformal mapping technique. The contribution of the center strip and ground plane to the kinetic inductance can be written separately as

$$L_{\text{kin1}} = \frac{\mu_0 \lambda_L C}{4ADK(k_0)} \times \frac{1.7}{\sinh\left(\frac{t}{2\lambda_L}\right)} \quad (68)$$

$$L_{\text{kin2}} = \frac{\mu_0 \lambda_L C}{4ADK(k_0)} \times \frac{0.4}{\sqrt{\left[\left(\frac{B}{A}\right)^2 - 1\right]\left[1 - \left(\frac{B}{D}\right)^2\right]}} \quad (69)$$

$$A = -\frac{t}{\pi} + \frac{1}{2} \sqrt{\left(\frac{2t}{\pi}\right)^2 + s^2} \quad (70)$$

$$B = \frac{s^2}{4A} \quad (71)$$

$$C = B - \frac{t}{\pi} + \sqrt{\left(\frac{t}{\pi}\right)^2 + w^2} \quad (72)$$

$$D = \frac{2t}{\pi} + C. \quad (73)$$

Based on (68) and (69), one can calculate the corresponding resistance of the center strip and ground plane by using (9) and (10). Now the total series inductance and resistance for all three types of superconducting, normal and hybrid CPWs can be found by using table 1.

Similar to the capacitance, the external inductance for all configurations is the same as in the case of having a perfect conductor. Consequently, by calculating the series inductance for the perfect conductor transmission line, we can use this value as an external inductance in other configurations, since fields cannot penetrate into a perfect conductor. When doing so, first we evaluate the characteristic impedance of the CPW line according to (74). Then we use the general relation (75) to find the external inductance of the line,

$$Z_0 = \frac{30\pi}{\sqrt{\varepsilon_{\text{ref}}^t}} \frac{k(k'_0)}{k(k_0)} \quad (74)$$

$$L_{\text{ext}} = Z_0^2 C. \quad (75)$$

In the case of having a dielectric loss, the shunt conductance associated with the line is

$$G = \omega C q \tan \delta \quad (76)$$

where the filling factor q is defined according to (57). As seen previously in table 1, the shunt conductance does not change for either the normal or superconducting state in all types of transmission lines.

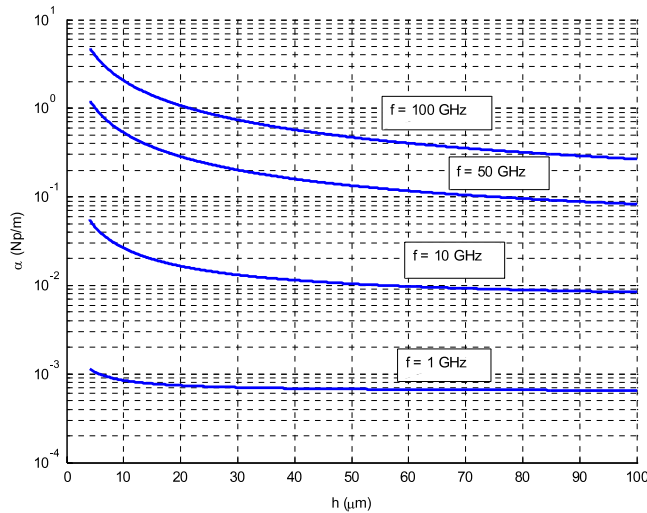


Figure 5. Attenuation constant (α) versus dielectric thickness (h) at various frequencies for superconducting PPTL. The dielectric spacer is liquid nitrogen and the superconductor is YBCO. These curves are in an excellent agreement with those obtained by full-wave analysis in [46].

6. Results

In practice, when a TL is to be designed and used for a specific purpose, one should choose the type, materials, dimensions of the TL and also the operating frequency. The type and configuration of the TL structure as well as the driven frequency are mostly determined by the application under study, device constraints and physical restrictions. The technology of fabrication can also impose limitations on the constituent materials of the structure including the substrate, metal, insulator and superconductor. Usually, the size and dimension of the structure is a factor that can be changed by a designer to achieve a particular functionality. Therefore, after choosing the type and configuration of TL, the inputs to the CAD tool are the materials characteristics, dimensions, temperature and frequency of operation. The CAD tools, in turn, calculate the circuit parameters associated with the TL. The outputs of the CAD tool will be the phase constant, attenuation constant, characteristic impedance, phase and group velocity which monitor the performance of a propagating wave through the TL. In this section, the results of applying the above described CAD tool to all configurations of PPTL, μ TL and CPW structures are shown and discussed.

For the superconducting PPTL illustrated in figure 2, the materials and geometrical parameters are chosen from [46]. The dielectric spacer is liquid nitrogen with $\epsilon_r = 1.454 - j7.27 \times 10^{-5}$. The superconductor plate is made of YBCO with critical temperature $T_c = 92$ K, penetration depth $\lambda_L(0) = 140$ nm and normal state DC conductivity of $\sigma_0 = 1.7 \times 10^6$ S m⁻¹. The thickness and width of each plate are $t = 760$ nm and $w = 10h$, respectively, where h is the height of the dielectric. The temperature is held at $T = 77$ K. The attenuation constant associated with a superconducting PPTL at various frequencies versus dielectric thickness (h) is shown in figure 5. This figure demonstrates that by increasing the

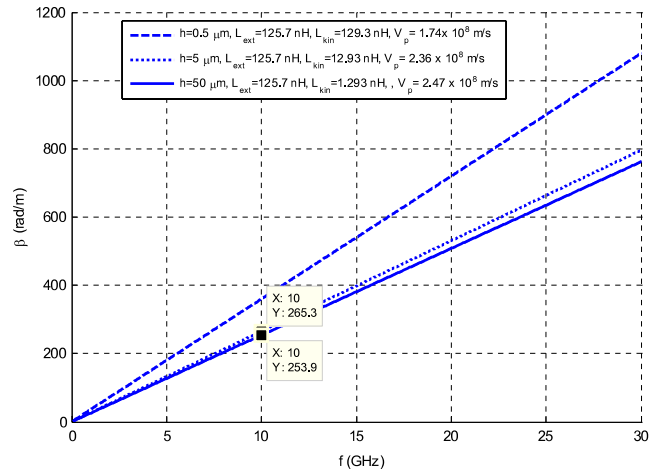


Figure 6. The effect of kinetic inductance on slow wave propagation in a superconducting parallel plate transmission line. The capture points in the figure are exactly the same as those obtained with full-wave analysis [46].

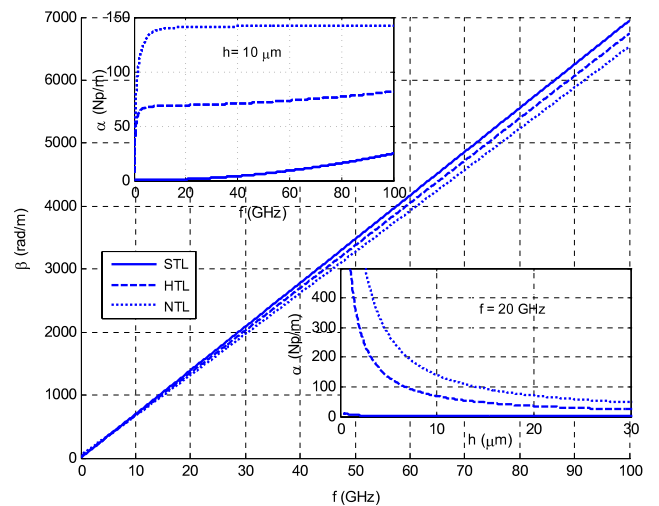


Figure 7. Dispersion diagram (β versus f) when $h = 10 \mu\text{m}$, distortion diagram (α versus f) and attenuation (α) versus dielectric thickness (h) for STL, HTL and NTL parallel plate TL. The superconductor is YBCO, the normal conductor is copper and the dielectric is MgO with $\epsilon_r = 9.65$.

dielectric thickness, the loss decreases, and after a particular value of h it remains unchanged. The results are in excellent agreement with those calculated by full-wave analysis in [46]. Moreover, its phase constant versus frequency (dispersion diagram) for different dielectric thickness are depicted in figure 6. The dispersion diagrams in this figure are linear as we consider a TEM transmission line. Equation (14) reveals the fact that decreasing h results in increasing L_{kin} , which slows down the wave propagation through the structure. This fact can be easily seen in figure 6. We captured two different points in this figure and compared them to the corresponding values in the table of [46]; they are exactly the same. The attenuation and phase constants of STL, HTL and NTL parallel plate TL are depicted in figure 7. The thickness of superconductor and normal conductor plates are taken as

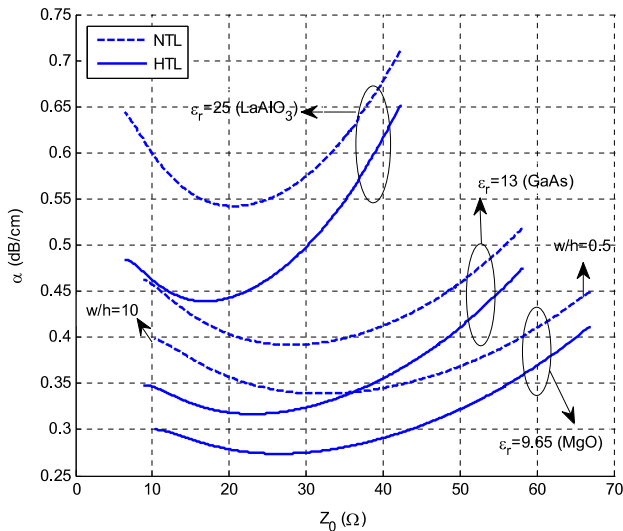


Figure 8. Attenuation constant (α) in terms of characteristic impedance (Z_0) for HTL and NTL microstrip TLs are plotted for different dielectric materials. By changing the aspect ratio (w/h) of a μ TL, these curves are generated. Other parameters are $f = 20$ GHz, $t = 3$ μ m, $h = 100$ μ m and $0.5h \leq w \leq 10h$. The curve corresponding to NTL with GaAs dielectric are in good agreement with the result in [11]. The superconductor is YBCO and the normal conductor is copper.

$t = 100$ nm and the dielectric spacer is MgO with $\epsilon_r = 9.65$. The superconductor is YBCO with characteristics mentioned above and the normal conductor is copper with conductivity of $\sigma_{nc} = 5.8 \times 10^7$ S m^{-1} . All other parameters are pointed out in the figure. Due to the presence of the superconductor material in STL and partially in HTL, attenuation constants associated with STL, HTL and NTL are expected to be the lowest, moderate and highest, respectively, as observed in figure 7. Furthermore, figure 7 shows that STL, HTL and NTL configurations exhibit different phase velocities from lower to higher, respectively. This is due to the existence of kinetic inductance in superconductor films.

Figure 8 illustrates the profiles of the attenuation constant for HTL and NTL microstrip TLs shown in figure 3 with respect to its corresponding characteristic impedance. These profiles are calculated by letting the aspect ratio (w/h) vary from 0.5 to 10 and then plotting α versus Z_0 . We omit the plot for STL μ TL, since it is located very close to the Z_0 axis due to the small amount of loss. Also, we repeat the plot of each curve for three different dielectric materials: LaAlO₃, GaAs and MgO with dielectric constants of $\epsilon_r = 25, 13$ and 9.65 , respectively. The superconductor material is YBCO and the normal conductor is copper with characteristics similar to those mentioned for PPTL. Other parameters are chosen from [11] such that $f = 20$ GHz, $t = 3$ μ m and $h = 100$ μ m. The width of the top strip changes from $0.5h$ to $10h$. This figure suggests that a μ TL is not suitable when a high impedance TL is demanded, because the right part of each curve in figure 8 grows fast and therefore the width of the top strip shrinks rapidly to zero. Moreover, attenuation constant associated with HTL always falls below the corresponding value for NTL, since the amount of loss is negligible in the superconductor

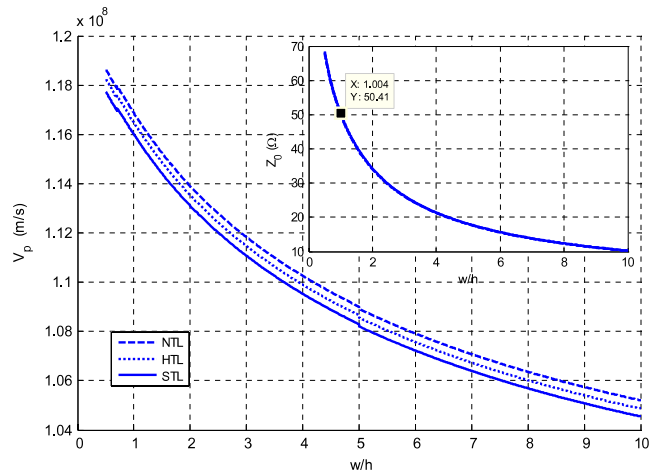


Figure 9. Phase velocity and characteristic impedance of STL, HTL and NTL microstrip TL versus its aspect ratio. The superconductor is YBCO, the normal conductor is copper and the dielectric is MgO. Other parameters are $f = 20$ GHz, $t = 100$ nm, $h = 100$ μ m and $0.5h \leq w \leq 10h$.

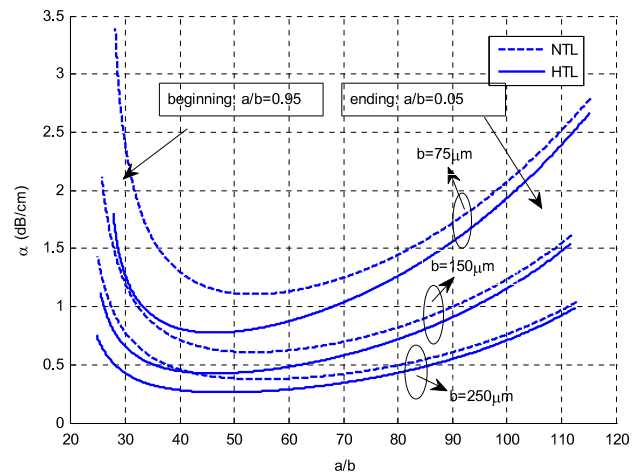


Figure 10. Variation of attenuation constant versus characteristic impedance on changing the aspect ratio of the CPW to $b = 75, 150$ and 250 μ m. The superconductor and conductor are YBCO and copper with a thickness of $t = 3$ μ m. The dielectric substrate is GaAs with $\epsilon_r = 13$ and thickness $h = 100$ μ m.

materials which HTL partially consists of. The profile of NTL with a GaAs dielectric are the same as the one shown in [11].

For the purpose of designing a μ TL with particular characteristic impedance, say 50 Ω , we need to calculate the characteristic impedance versus aspect ratio. This task is performed in figure 9, and the desired aspect ratio is found to be close to 1 for $Z_0 = 50$ Ω μ TL. Parameters of the μ TL are written below the figure. This figure also demonstrates that there is no difference between STL, HTL and NTL from a characteristic impedance point of view. Moreover, the phase velocities of these three configurations of μ TLs are compared in figure 9 at a frequency of 20 GHz. As explained before, the phase velocity of STL, HTL and NTL are ordered from low to high, respectively.

The same profiles are plotted in figures 10 and 11 when the transmission line is a typical CPW illustrated in figure 4.

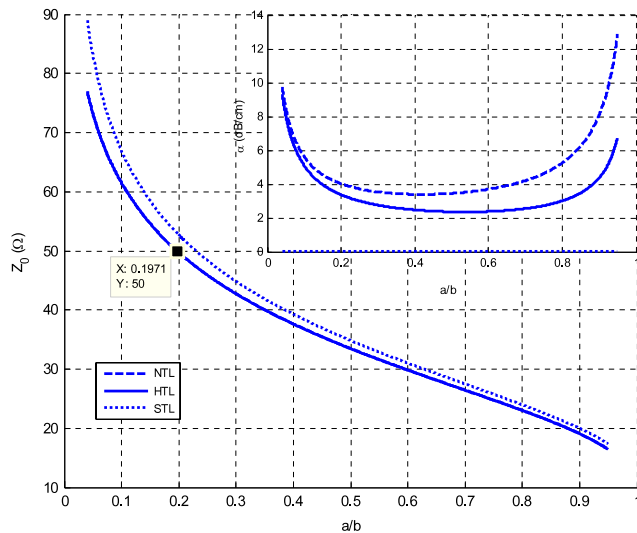


Figure 11. The profile of characteristic impedance and attenuation constant with respect to the aspect ratio for STL, HTL and NTL CPW lines. The superconductor and conductor are TI-2212 and copper with a thickness of $t = 100$ nm. The dielectric substrate is LaAlO_3 with $\epsilon_r = 25$ and a thickness of $h = 500$ μm . Parameter b is fixed at $b = 100$ μm .

Superconductor plates, normal conductor plates and dielectric substrate in figure 10 are made of YBCO, copper and GaAs, respectively, with the same characteristics mentioned for PPTL. However, the superconductor material in figure 11 is TI-2212 with parameters $T_c = 110$ K, $\lambda_L(0) = 300$ nm and $\sigma_0 = 2.85 \times 10^4$ S m^{-1} . The normal conductor and dielectric is copper and LaAlO_3 with $\epsilon_r = 25$ in figure 11. The thicknesses of the plates and dielectric are assumed to be $t = 3$ μm and $h = 100$ μm and $t = 100$ nm and $h = 500$ μm in figures 10 and 11, respectively.

In figure 10, the attenuation constant versus characteristic impedance is depicted, as the aspect ratio varies from 0.05 to 0.95. We assumed that b ($b = s + 2w$) is fixed for each curve and the width of center strip ($a = s$) varies. NTL profiles in this figure are in agreement with those in [11]. As mentioned for PPTL and μTL , the HTL exhibits a smaller loss compared to the NTL as observed in figure 10. A detailed observation of this figure suggests that the CPW is not suitable for realization of low impedance TLs, while it is suitable to achieve high impedance lines. The reverse statement is valid for μTL s, as pointed out in the previous paragraph.

The profiles of characteristic impedance and attenuation constant are shown in figure 11. We used this profile to design a 50 Ω CPW. Also, small and high values of aspect ratio create a huge amount of loss as observed in the attenuation profile in this figure. As expected, the attenuation constant corresponding to a STL is located very close to the zero value.

7. Conclusion

A microwave CAD tool was proposed to be used for the fast analysis and design of parallel plate, microstrip and CPW transmission lines with various configurations of superconductor, normal conductor and hybrid transmission

line. Since closed-form equations have not been reported for every circuit parameter of a transmission line, we used the concept of surface impedance associated with a plate of conductor with finite thickness. The novelty of this work mostly relies on the method of finding closed-form equations for the hybrid transmission line, based on the reported CAD formula in literature. All the necessary equations to find the circuit parameters of all three TLs have been listed in this paper. The results of the simulation of particular structures which are useful for design purposes were presented in the last section of the paper based on the CAD tool developed.

References

- [1] Lancaster M J 1997 *Passive Microwave Device Applications of High-Temperature Superconductors* (Cambridge: Cambridge University Press)
- [2] Orlando T P and Delin K A 1990 *Foundations of Applied Superconductivity* (Massachusetts: Addison-Wesley)
- [3] HYPRES, Inc. <http://www.hypres.com/>
- [4] National Institute of Standards and Technology <http://www.nist.gov/>
- [5] Yurke B *et al* 1989 Observation of parametric amplification and deamplification in a Josephson parametric amplifier *Phys. Rev. A* **39** 2519–35
- [6] Castellanos-Beltran M A and Lehnert K W 2007 Widely tunable parametric amplifier based on a superconducting quantum interference device array resonator *Appl. Phys. Lett.* **91** 083509
- [7] Majedi A H, Chaudhuri S K and Safavi-Naeini S 2001 Optical-microwave interaction modeling in high-temperature superconducting films *IEEE Trans. Microw. Theory Tech.* **49** 1873–81
- [8] Zhizhong Y and Majedi A H 2007 Physical modeling of hot-electron superconducting single-photon detectors *IEEE Trans. Appl. Supercond.* **17** 3789–94
- [9] DiVincenzo D P 2000 The physical implementation of quantum computation *Fortschr. Phys.* **48** 771–83
- [10] Collin R E 1992 *Foundations for Microwave Engineering* (New York: McGraw-Hill)
- [11] Gupta K C, Garg R, Bahl I and Bhartia P 1996 *Microstrip Lines and Slotlines* (Boston, MA: Artech House Publishers)
- [12] Wadell B C 1991 *Transmission Line Design Handbook* (Boston, MA: Artech House Publishers)
- [13] Chang W H 1979 The inductance of a superconducting strip transmission line *J. Appl. Phys.* **50** 8129–34
- [14] Rauch W and Gornik E 1993 Microwave properties of $\text{YBa}_2\text{Cu}_3\text{O}_{7-x}$ thin films studied with coplanar transmission line resonators *J. Appl. Phys.* **73** 1866–72
- [15] Yassin G and Withington S 1995 Electromagnetic models of superconducting millimetre-wave and sub-millimetre-wave microstrip transmission lines *J. Phys. D: Appl. Phys.* **28** 1983–91
- [16] Wheeler H A 1977 Transmission-line properties of a strip on a dielectric sheet on a plane *Microw. Theory Tech.* **25** 631–47
- [17] Tang W C and Chow Y L 2001 CAD formula and their inverses for microstrip, CPW and conductor-backed CPW by successive synthetic asymptotic *Antennas and Propagation Society (Boston)* vol 3 pp 394–7
- [18] Hammerstad E and Jensen O 1980 Accurate models for microstrip computer-aided design *Microwave Symp. Digest (Washington)* vol 80 pp 407–9
- [19] Yamashita E and Atsuki K 1979 An approximate dispersion formula of microstrip lines for computer aided design of microwave integrated circuits *Microwave Symp. Digest (Orlando); IEEE Trans. Microw. Theory Tech.* **79** 320–2
- [20] Getsinger W J 1973 Microstrip Dispersion Model *Microw. Theory Tech.* **21** 34–9

- [21] Kobayashi M 1988 A dispersion formula satisfying recent requirements in microstrip CAD *Microw. Theory Tech.* **36** 1246–50
- [22] Van Duzer T and Turner C W 1999 *Principles of Superconductive Devices and Circuits* (Englewood Cliffs, NJ: Prentice-Hall)
- [23] www.cryo.eecs.berkeley.edu/CADtools.html
- [24] Agilent Technology, Advanced Design System (ADS) http://adsabs.harvard.edu/abs_doc/help_pages/
- [25] Ansoft 3D Full-wave Electromagnetic Field Simulation (HFSS) <http://www.ansoft.com/products/hf/hfss/>
- [26] <http://www.wrcad.com/wrspice.html>
- [27] Polonsky S V, Semenov V K and Shevchenko P N 1991 PSCAN: personal superconductor circuit analyser *Supercond. Sci. Technol.* **4** 667–70
- [28] <http://www.sonnetusa.com/>
- [29] Zeland Software product IE3D. <http://www.zeland.com/>
- [30] Computational Prototyping Group at MIT. http://www.rle.mit.edu/cpg/research_codes.htm
- [31] <http://www.fastfieldsolvers.com/>
- [32] Mohebbi H R and Majedi A H 2007 Characteristics of superconducting transmission line with metal grating for microwave circuits *ISSSE 2007: IEEE, Int. Symp. on Signals, Systems and Electronics (Montreal, QC)* pp 213–6
- [33] Mohebbi H R and Majedi A H 2009 Periodic superconducting microstrip line with nonlinear kinetic inductance *IEEE Trans. Appl. Supercond.* **19** 930–5
- [34] Mohebbi H R and Majedi H A 2009 Analysis of series-connected discrete Josephson transmission line *IEEE Trans. Microw. Theory Tech.* **57** 1865–73
- [35] Popzar D 2005 *Microwave Engineering* (Hoboken, NJ: Wiley)
- [36] Mohebbi H R, Shaker J, Chaharmir M R and Sebak A R 2006 Mode matching and point matching techniques for dispersion curves of microstrip line structures *ANTEM (Montreal, QC)* pp 197–200
- [37] Mittra R and Itoh T 1971 A new technique for the analysis of the dispersion characteristic of microstrip lines *IEEE Trans. Microw. Theory Tech.* **19** 47–56
- [38] Senior T B A and Volakis J 1995 *Approximate Boundary Conditions in Electromagnetics* (London: Institution of Electrical Engineers)
- [39] Jordan E C and Balmain K G 1968 *Electromagnetic Waves and Radiating Systems* (Englewood Cliffs, NJ: Prentice-Hall)
- [40] Hanson G W and Yakovlev A B 2002 *Operator Theory for Electromagnetics: An Introduction* (New York: Springer)
- [41] Wu C-J and Tseng T-Y 1996 Microwave surface impedances of BCS superconducting thin films *IEEE Trans. Appl. Supercond.* **6** 94–101
- [42] Vendik O S, Vendik I B and Kaparkov D I 1998 Empirical model of the microwave properties of high-temperature superconductors *Microw. Theory Tech.* **46** 469–78
- [43] Yoshida k, Mohammad Sajjad H, Kisu T, Enpuku K and Yamafuji K 1992 Modeling of kinetic-inductance coplanar stripline with NbN thin film *Japan. J. Appl. Phys.* **31** 3844–50
- [44] Jackson J D 1963 *Classical Electrodynamics* (New York: Wiley)
- [45] Barone A and Paterno G 1982 *Physics and Applications of the Josephson Effect* (New York: Wiley)
- [46] Wu C J 2001 Microwave propagation characteristics of a high-temperature superconducting variable spacing parallel plate transmission line *J. Appl. Phys.* **89** 3986–92
- [47] Farhat A, Davis L E and Gallop J C 1993 Field solution for a thin-film superconducting parallel-plate transmission line *Physica C* **215** 132–44
- [48] Zhou S-A 1999 *Electrodynamics of Solids and Microwave Superconductivity* (New York: Wiley)
- [49] Melkov G A and Egorov Y V 2000 Swihart waves and surface plasmons in a parallel-plate superconducting transmission line *Low Temp. Phys.* **26** 108–14
- [50] Itoh T 1987 *Planar Transmission Line Structures* (New York: IEEE Press)
- [51] Kirschning M and Jansen R H 1984 Accurate wide-range design equations for the frequency-dependent characteristic of parallel coupled microstrip lines *Microw. Theory Tech.* **32** 83–90
- [52] Kirschning M, Jansen R H and Koster N H L 1983 Measurement and computer-aided modeling of microstrip discontinuities by an improved resonator method *IEEE MTT-S International Microwave Symposium Digest (Boston)* pp 495–7
- [53] Simons R N 2001 *Coplanar Waveguide Circuits, Components, and Systems* (New York: Wiley)
- [54] Hasnain G, Dienes A and Whinnery J R 1986 Dispersion of picosecond pulses in coplanar transmission lines *IEEE Trans. Microw. Theory Tech.* **34** 738–41
- [55] Valenzuela A A, Solkner G, Kessler J and Russer P 1993 Microwave characterisation of structured $\text{YBa}_2\text{Cu}_3\text{O}_{7-x}$ -thin films *Mater. Sci. Forum* **130–132** 349–72